

A Comparison of Quasi-Static Characteristics and Failure Signatures of GMR Heads subjected to CDM and HBM ESD Events

Chris Moore

Integral Solutions, Int'l, 2192 Bering Drive, San Jose, CA 95131 408-941-8300; cmoore@isiguy.com

Abstract— The effects of the Human Body Model (HBM) Electro-Static Discharge (ESD) waveform on Giant Magneto-Resistive (GMR) heads is fairly well characterized. This information provides a baseline against which a comparison can be made for other ESD models. The goal of this work is to compare and contrast the effects that are seen in GMR sensors when they are subjected to the Charged-Device Model (CDM) versus HBM ESD events. This study compares the effects of CDM waveforms versus HBM waveforms on a single design of MR head. Although the HBM waveform has provided a starting point for understanding ESD damage to GMR heads, it is believed that the CDM model has a more useful basis in the reality of head manufacturing. This makes study of the effects of CDM ESD events on GMR heads both important and interesting. Detailed characterization of head response as a function of the ESD waveform was realized using a new system combining quasi-static (QST) analysis with in-situ CDM and HBM ESD simulation capabilities. A SEM was used to perform failure analysis on damaged heads in an attempt to characterize differences in the ‘failure signature’ of the sensor.

Introduction

There exists a significant body of work related to studying the effects that Electro-Static Discharge (ESD) events have on Giant Magneto-resistive (GMR) heads. This work is important due to the extreme sensitivity of these devices to uncontrolled current transients.¹ The integration of ESD simulators with test systems designed to characterize the magnetic and electrical response of a GMR element has been done in the laboratory as well as at the commercial level. Simulations of ESD events used in research have typically been limited to the Human Body Model (HBM) or Machine Model (MM) events for which there exist documented standards and a reasonably simple ability to integrate these waveform simulators with test equipment. Although these are the most commonly utilized waveforms, they may not be the most accurate way to model those events that threaten the GMR element in the manufacturing environment. There is a growing interest in using a simulated waveform that can emulate the extremely fast and high current amplitude event which occurs when a charged device makes contact with body at a different

potential. The Charged Device Model (CDM) is designed to simulate this type of contact.

Until recently there have been only a handful of studies related to CDM events and GMR heads. Some examples of these studies can be found in references 2 and 3. One reason for the limited amount of research in this area may be the comparative difficulty of interleaving the production of a controlled CDM event through a GMR element with the evaluation of this element between CDM events. The introduction of a commercially available in-situ CDM ESD simulator and Quasi-Static Test (QST) System allows a more detailed characterization of GMR heads subjected to this type of transient event.

The response of GMR elements to HBM ESD events is well documented.⁴ This provides a benchmark for comparing the results of CDM characterization of GMR heads.

Experimental Setup

The experimental setup consisted of the following components:

- 1) Quasi-static (QST) tester
- 2) In-situ HBM ESD Simulator
- 3) In-situ CDM ESD Simulator
- 4) Tektronix CT-6 2GHz AC Current Probe
- 5) LeCroy 9362 1.5GHz 10GS/s Digital Scope

A quasi-static test environment was most appropriate for this experiment since GMR heads display both magnetic and resistive degradation as a function of ESD.⁴ The Integral Solutions (ISI) QST-2001 was used to provide quasi-static measurements of the heads. Two QST-2001 system peripherals were used to supplement the test environment with ESD capabilities. The ISI HBM ESD Waveform Simulator and the ISI CDM ESD Waveform Simulator provided fully software controlled and integrated injection of ESD transients into the GMR element.⁵

A single type of conventional spin-valve GMR head was used for this study. The design was a 5 GB/in² GMR sensor with a PtMn exchange layer.

Test Conditions

Data was collected on six heads under the following conditions:

Stress	HBM	CDM
Bias	+5mA	+5mA
Transfer Curve Field Strength (Oe)	+/- 100	+/- 100
Test Termination Point	2%,5%,10% Resistance Change	2%,5%,10% Resistance Change
Course Voltage Increment	5V	2V
Fine Voltage Increment	2V	2V
Pulse Polarity Per Voltage	Pos – Neg	Pos – Neg

Table 1. Test conditions.

Testing Procedure

Six heads were subjected to ESD step stress testing until failure. Three heads were stressed with an HBM waveform and three heads were stressed with a CDM waveform. Percentage change in resistance was used as the failure criteria to terminate the testing sequence. The first HBM stressed head was tested until there was a 2% change in resistance, the second tested until there was a 5% change in resistance, and the third head was tested until there was a 10% change in resistance. This same sequence was used in testing the CDM heads. This selection of percentage resistance changes was chosen to facilitate the identification of failure signatures during SEM analysis. It was believed that a head tested to complete resistance failure was less likely to have a useful and distinct visual signature than one tested to partial failure.

During HBM step stress testing the incremental voltage below 20V was in 5V steps. Above 20 volts the incremental voltage was in 2V steps. During CDM testing 2V increments were used throughout testing. For all stress sequences at each voltage the head was stressed with a positive pulse followed by a negative pulse of the same magnitude.

The amplitude and slope of the transfer curve and the resistance of the sensor were selected as the primary parameters to monitor for changes as a function of injected ESD.

Nomenclature Definition

The nomenclature utilized in the graphing of data will be as follows:

[Waveform][% Resistance at Failure][Pulse Polarity]

An example of this would be **H10P**, representing data from a head tested using the [H]BM waveform, with testing terminated at **10%**, from a [P]ositive pulse.

HBM Test Results

Figure 1 is a summary of head resistance versus V_{HBM} for the three heads tested with the HBM simulator. This head design shows initial resistance change at a V_{HBM} of between 35V and 38V with more serious resistance changes occurring after 40V. **Figures 3 to 5** are plots of peak to peak transfer curve amplitudes as a function of V_{HBM} for these three heads.

In each of these plots it is possible to observe the characteristic polarity toggling commonly associated with HBM testing of GMR heads. This pattern is most clearly represented in **Figure 5**. This phenomenon is the result of a reversal in the pinned-layer during alternate polarity transients through the GMR sensor. Above a threshold V_{HBM} the pinned-layer is quickly heated beyond the blocking temperature. The current transient that causes the heating also generates a magnetic field of sufficient strength to set or reset the pinned-layer before it cools below the blocking temperature. Thus, above a critical voltage, the polarity of the transfer curve will toggle when the polarity of the HBM event is reversed.⁴

CDM Test Results

Figure 2 is a summary of head resistance versus plate voltage for the three heads tested with the CDM simulator. This sensor design shows an initial resistance change at plate voltages ranging from 28V to 34V.

Figures 6 to 8 show the peak to peak transfer curve amplitudes of these same heads as a function of plate voltage. Of special interest is that, unlike heads subjected to an HBM step stress, no well-defined pinned-layer toggling occurs after the initial reversal occurs.

Figure 6, which represents the CDM 2% resistance change data, is the closest in appearance to the behavior seen with the HBM simulator. This head has a consistent pinned-layer reversal on each successive reverse polarity ESD signal injection. This series of reversals takes place only after the initial inversion of the pinned-layer at 28V. This inversion takes place on the +28V signal and remains during the -28V signal. It is then the +30V signal that returns the pinned-layer to its original configuration. **The same polarity signal caused both an inversion and a**

return to the original pinned-layer orientation! This behavior is quite different than that seen during HBM testing. Pinned-layer reversal consistently occurs on successive and **alternating** polarity ESD events. **Figures 6 to 8** offer no consistent pattern for predicting when the pinned-layer will reverse when the head is subjected to a CDM event.

Comparison of HBM versus CDM Results

Figure 9 shows normalized resistance versus V_{HBM} for the three heads subjected to the HBM waveform. **Figure 10** shows normalized resistance versus plate voltage for the three heads subjected to the CDM waveform. From these two graphs it is clear that the CDM results show resistance changing more rapidly versus stress voltage, with less than 2V from the onset of resistance change to a greater than 10% resistance change. The equivalent change in resistance for HBM testing occurs at no less than 4V.

Because resistance change is occurring as a function of injected current, not specifically charge voltage, it is important to look more closely at the peak current values through the GMR sensor. It is noted that the CDM simulator produces a 4.1mA/1V increase in current for this head design. The HBM simulator produces a 0.65mA/1V increase in current. Thus a 1 to 2V difference in CDM voltage is a 4.1mA to 8.2mA change in stress current through the head. The 4V+ change in HBM voltage is a 2.6mA+ in stress current through the head. **Figure 11** is the HBM normalized resistance data versus stress current and **Figure 12** is the corresponding CDM data. From these two plots it becomes apparent that the HBM simulator produces a more rapid change in resistance as a function of stress current. These two plots are also useful in demonstrating the difference in resistance failure

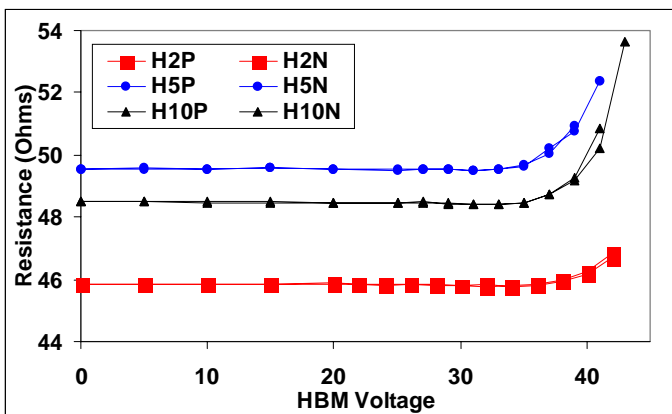


Figure 1: Resistance vs HBM Voltage

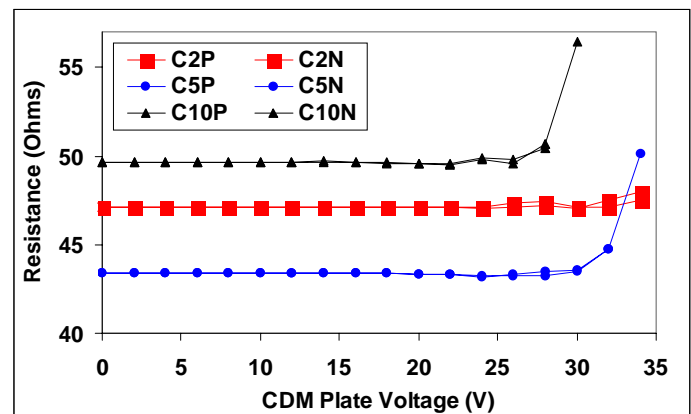


Figure 2: Resistance vs CDM Plate Voltage

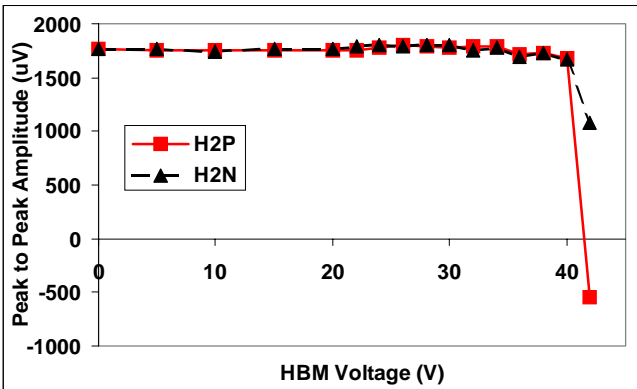


Figure 3: Peak to Peak Amplitude vs HBM Voltage: 2% Failure Point

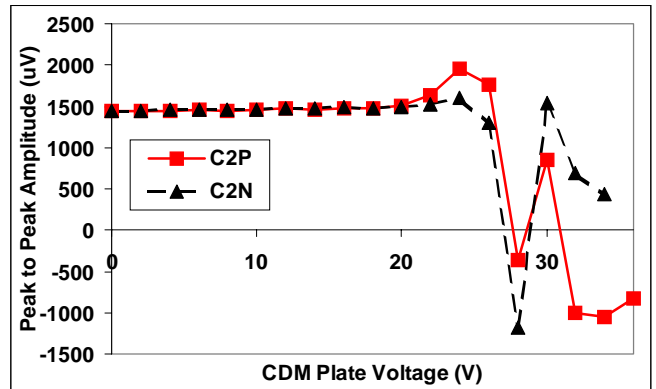


Figure 6: Peak to Peak Amplitude vs CDM Plate Voltage: 2% Failure Point

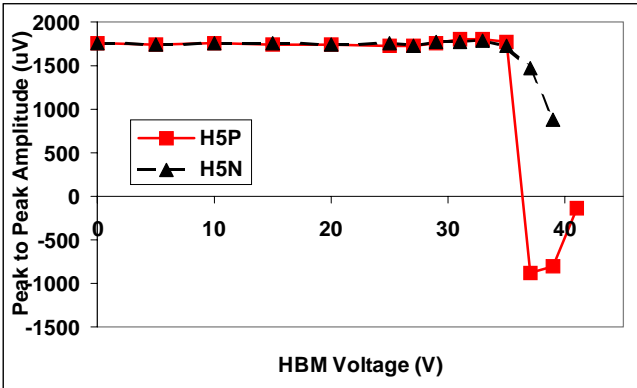


Figure 4: Peak to Peak Amplitude vs HBM Voltage: 5% Failure Point

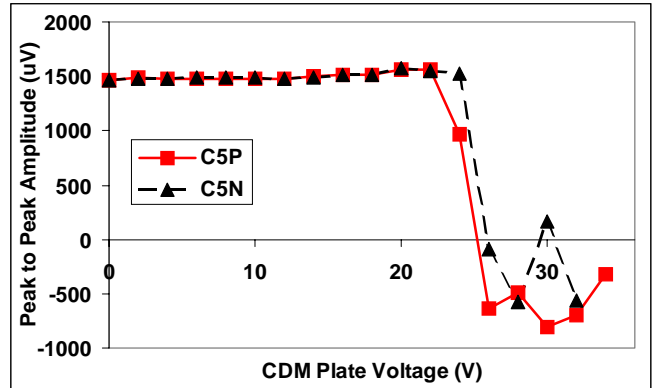


Figure 7: Peak to Peak Amplitude vs CDM Plate Voltage: 5% Failure Point

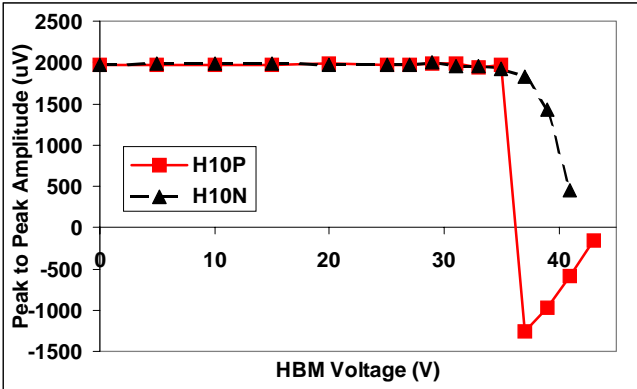


Figure 5: Peak to Peak Amplitude vs HBM Voltage: 10% Failure Point

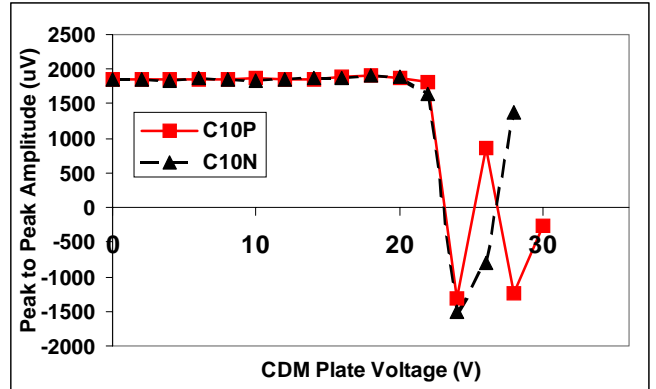


Figure 8: Peak to Peak Amplitude vs CDM Plate Voltage: 10% Failure Point

currents between the two ESD models. The **HBM** resistance failure point occurred around **22mA to 24mA** and the **CDM** resistance failure point occurred around **115mA to 140mA**.

Figure 13 shows the normalized peak to peak amplitudes versus V_{HBM} for the three heads subjected to the HBM waveform. **Figure 14** shows normalized peak to peak amplitude versus plate voltage for the CDM data. The HBM data in **Figure 13** shows that

changes in peak to peak amplitude first appear in the V_{HBM} range of 35V to 38V. The corresponding range in sensor current for these V_{HBM} values is from 22.75mA to 24.7mA. The CDM data in **Figure 14** shows a surprisingly consistent critical initial failure point at a plate voltage of 22V. This plate voltage corresponds to a peak sensor current of 90mA. **Figure 15** shows the actual waveform through a head at a plate voltage of 22V.

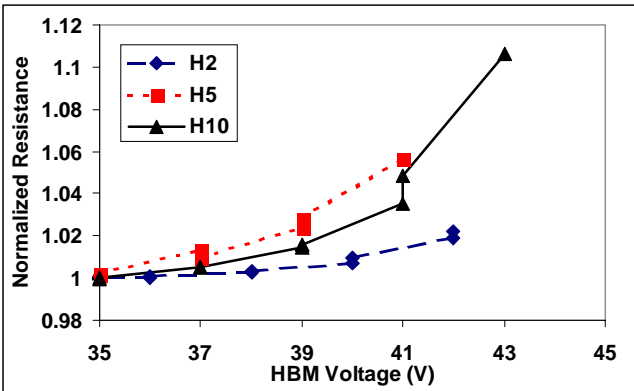


Figure 9: Normalized Resistance vs HBM Voltage

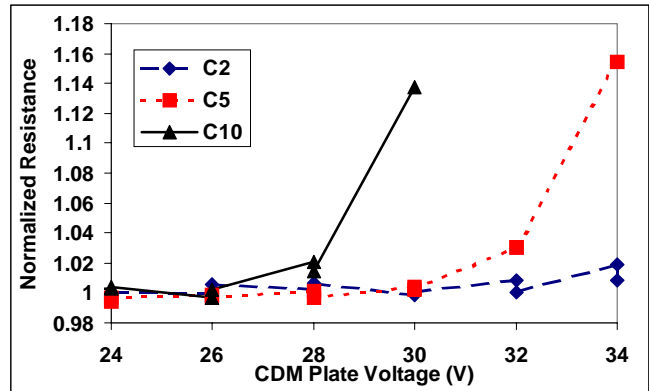


Figure 10: Normalized Resistance vs CDM Plate Voltage

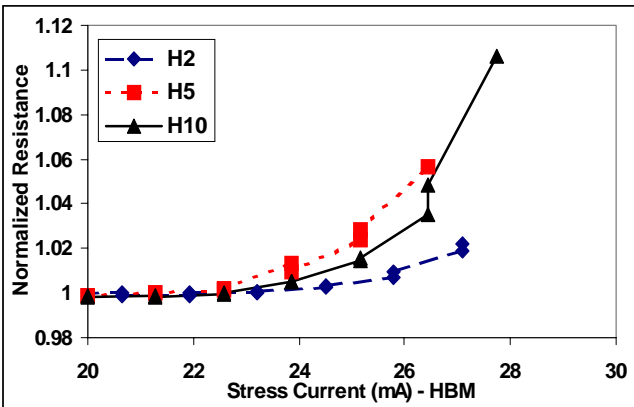


Figure 11: Normalized Resistance vs HBM Stress Current

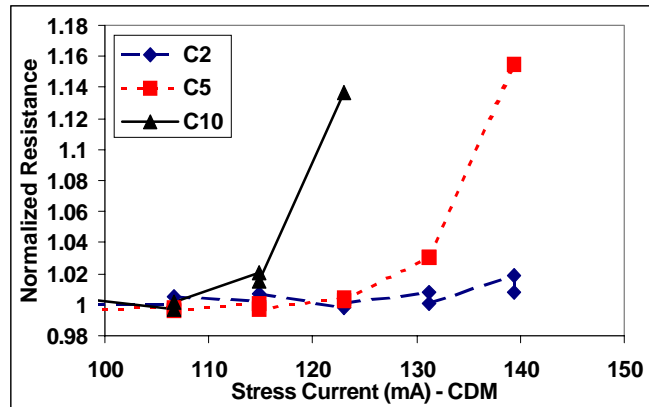


Figure 12: Normalized Resistance vs CDM Stress Current

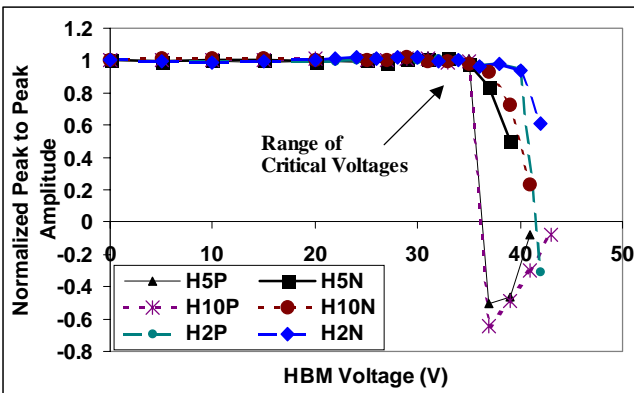


Figure 13: Normalized Peak to Peak Amplitudes vs HBM Voltage

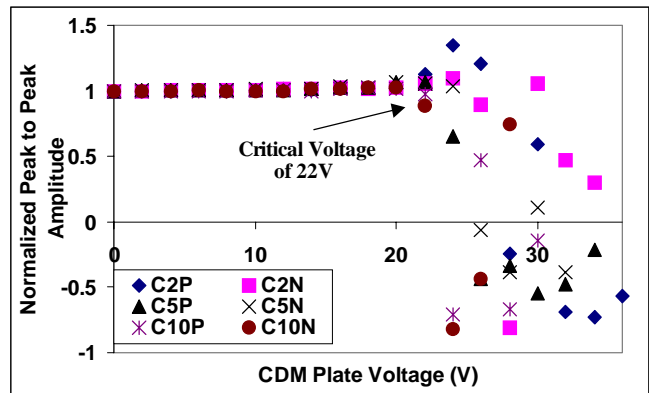


Figure 14: Normalized Peak to Peak Amplitude vs CDM Plate Voltage

SEM Results

At the time of publication the SEM results for these six heads were not available. The presentation on this material given at the 2000 EOS/ESD Symposium is available at the following web location: <http://www.isiguy.com/PublishedArticles.htm>. This

presentation provides the SEM results for the heads discussed in this paper. Supplemental information on the testing of additional head designs may also be available.

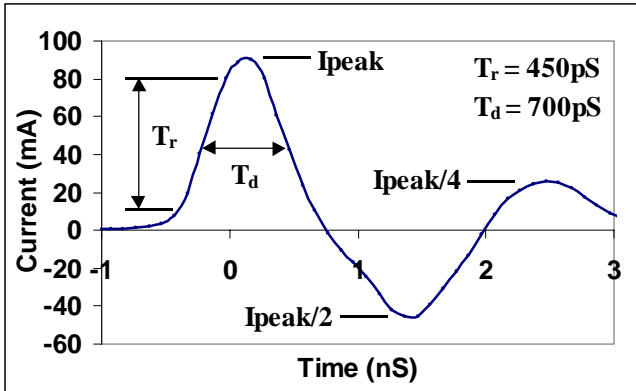


Figure 15: +22V CDM Waveform Through Head

References

- [1] A. Wallash, "Electrostatic Discharge (ESD) in Magnetic Recording: Past, Present, and Future", Presented at the 2000 ESDDiscovery 2000, www.wallash.com.
- [2] A. Wallash and Y.K. Kim , "Electrostatic Discharge Sensitivity of Giant Magnetoresistive Recording Heads", Journal of Applied Physics, 15 April 1997.
- [3] A. Wallash, "Field Induced Charged Device Model Testing of Magneto-resistive Recording Heads", Proc. 18th EOS/ESD Symp. (1996), pp. 8-13.[15].
- [4] A. Wallash and Y.K. Kim, "Magnetic Changes in GMR Heads caused by Electrostatic Discharge", IEEE Trans. Magn., VOL. 34, NO. 4. July 198, pp. 1519-21.
- [5] Integral Solutions International, San Jose, CA. (408) 941-8300. Tester model QST 2001 with HBM and CDM ESD Simulators.

Summary of Results

- 1) HBM stress causes permanent changes in resistance over a shorter range of current than does CDM stress.
- 2) CDM stress testing does not produce as predictable an effect on the pinned-layer as does the HBM stress pattern of alternating pinned-layer reversal.
- 3) The design of GMR sensor used in this experiment is 3.5 to 4 times less sensitive to a CDM current waveform than to an HBM current waveform.

Conclusion

This initial comparison of a single head design subjected to both HBM and CDM ESD events shows that the GMR element reacts quite differently to these two types of waveforms. This difference is especially apparent in the magnetic response of the sensor and in the peak current tolerated by the head. It is believed that further study is both useful and necessary to fully understand the underlying mechanism behind the response of the GMR element to CDM events.

Acknowledgements

The author would like to acknowledge the invaluable assistance of Igor Gorin in the development of the prototype CDM waveform simulator and the enthusiastic support for this project by Dr. Al Wallash.